Journal of Natural Resources and Farming
https://doi.org/10.7770/jonraf-v2-art2906

JONRAF Journal of Natural Resources and Farming

SPECIAL ISSUE

Reference-Based Model for Post-Irrigation Soil-Moisture Recovery in a Positive State Space

Gustavo A. Maldonado-Batres[a*], Marlon M. López-Flores[b], William Campillay-Llanos[c]

Escuela de Matemática y Ciencias de la Computación, Universidad Nacional Autónoma de Honduras (UNAH), Ciudad Universitaria, Tegucigalpa, D.C.[a], Honduras.
Laboratório de Inteligência Artificial, Robótica e Cibernética (LIARC), Instituto Militar de Engenharia (IME-RJ), Rio de Janeiro[b], Brazil.
Departamento de Ciencias Matemáticas y Físicas; Núcleo de Investigación en Producción Alimentaria (NIPA), Universidad Católica de Temuco, Temuco[c], Chile.

Article history
Received: 10/02/2026
Accepted: 14/07/2026
Published: 22/09/2026

Corresponding author
*Gustavo A. Maldonado-Batres
gustavo.batres@unah.edu.hn

ABSTRACT
Purpose. We develop a reference-based positive-state law to describe sensor-reported soil-moisture recovery after irrigation and evaluate its conditional empirical performance without claiming a hydraulic mechanism or universal superiority. **Methods.** The ratio θ/θ_{ref} was modeled in shifted dimensionless time by proportional relaxation. An open dataset from a single strawberry farm was processed through a single archived analysis pipeline. Flow increments greater than 5 L defined candidate irrigation records, and recovery fitting used the first contiguous sequence strictly above the event-specific reference. Proportional, additive-power, additive-exponential, and stretched-exponential curves were fitted to identical observations using log-ratio loss and evaluated by full-window diagnostics and a 70/30 elapsed-time hold-out. **Results.** Of 101 detected events, 36 met the restrictive criteria. Median full-window $RMSE_{log}$ was 0.00351 for the proportional curve, 0.00360 for additive power, 0.00597 for the exponential, and 0.00298 for the stretched exponential. The proportional curve outperformed the exponential and additive power in 32/36 events, but the stretched exponential had lower full-window error in 33/36. In ordered-time hold-out, proportional and stretched-exponential performance was evenly divided (18/36). **Conclusions.** The contribution is a positive, interpretable parameterization and a transparent, reproducible workflow rather than a uniquely best empirical curve. Calibrated sensors, uncertainty propagation, weather covariates, and multi-site external validation are required before operational use. Keywords: soil-moisture drydown; irrigation events; positive-state model; log-ratio error; model comparison; reproducible research

Keywords: soil-moisture drydown; irrigation events; positive-state model; log-ratio error; model comparison; reproducible research

1. Introduction

Soil moisture supports irrigation scheduling, crop-water planning, and sustainable management of water resources (Allen et al., 1998; Jones, 2004; Datta and Taghvaeian, 2023). Sensor records are positive, but their numerical values depend on device type, soil-specific calibration, installation, texture, and measurement depth (Topp et al., 1980; Bittelli, 2011; Ganjegunte et al., 2012; Vereecken et al., 2008). The open dataset used here reports a soil-moisture percentage without a supplied site-specific calibration that would justify calling it volumetric water content. We therefore use the term *sensor-reported soil-moisture percentage* throughout.

Mechanistic models such as the Richards equation are required when hydraulic conductivity, capillarity, redistribution, root uptake, and boundary fluxes must be resolved (Richards, 1931). Reduced event-level models address a different question: whether a compact curve describes the observed trajectory over a defined window. Soil-moisture drydown studies use exponential, nonlinear, and power-law-like forms, while segmentation and changepoints remain substantive parts of the analysis rather than neutral preprocessing (McColl et al., 2017; Sehgal et al., 2021; Raoult et al., 2021; Sinha et al., 2024; Gong et al., 2025).

This article considers a reduced response model for a positive state measured relative to an event-specific reference. In proportional arithmetic, the multiplicative identity 1 represents no relative deviation and logarithmic coordinates convert proportional operations into ordinary linear operations (Bashirov et al., 2008; Campillay-Llanos et al., 2021). The formulation does not assert that soil-water physics is intrinsically proportional. Its purpose is to encode recovery toward a positive reference, preserve positivity, and make ratio-type errors explicit.

A central methodological concern is that the proportional solution has a power-law tail in the logarithmic relative deviation. A comparison only against an additive exponential could therefore favor the proposed curve because of tail flexibility rather than because proportional coordinates are uniquely supported by the data. We address this directly by fitting four prespecified candidates to identical observations, including a freely estimated additive power law and a stretched exponential. This study develops the positive-state law and its ordinary equivalent, quantifies its conditional performance under one fully specified event-extraction protocol, and distinguishes representational value from empirical model ranking. No soil-hydraulic parameter, causal irrigation effect, or universal model superiority is claimed.

2. Materials and Methods

2.1 Study design, data source, and target estimand

The empirical component is a retrospective, event-level case study based on Version 3 of the open Mendeley Data record "Smart irrigation control system data with soil moisture, flow meter and electrovalve relay" (Manzano et al., 2023). It contains 4,293 moisture rows, 17,411 cumulative flow-meter rows, and 17,427 electrovalve-command rows collected from 12 July to 16 September 2022 at a single strawberry production farm in Itagua, Paraguay. The associated deployment article describes capacity-based moisture sensing in a cloud-connected irrigation system (Orihuela et al., 2025).

The estimand is the conditional trajectory after a flow-derived irrigation pulse, conditional on a detectable recovery that remains above an event-specific reference for a sufficient duration and has adequate sampling density. It is not the response of every irrigation pulse, a causal treatment effect, field capacity, or a transferable hydraulic coefficient.

2.2 Data cleaning, event extraction, and quality control

All timestamps were parsed as Coordinated Universal Time (UTC) and sorted. Non-finite rows were removed, and duplicate timestamps were resolved by retaining the last recorded value. One duplicate flow timestamp was detected, leaving 17,410 cleaned flow records. Negative cumulative-flow differences were flagged as counter resets or discontinuities and were not interpreted as irrigation. Large isolated positive increments were flagged for review rather than silently removed.

Candidate irrigation records were consecutive cumulative-flow increases greater than 5 L. Active records separated by no more than 15 min were merged, and the event end was defined as five minutes after the final active record. The 5 L threshold filters very small counter changes; its influence was evaluated at 0, 1, 5, and 10 L. Valve commands within ±10 min min of each event were summarized as an audit variable rather than an exclusion rule because the command and measured-flow logs were not assumed to be synchronous.

Events below 300 L were excluded. The reference θ_{ref} was defined as the median moisture during the six hours before the event start, with at least three observations required. The recovery origin was the observed maximum within three hours after irrigation ended. Starting from that peak, the fitted window was the first contiguous sequence with moisture strictly greater than θ_{ref}. It ended before the first observation at or below θ_{ref}, before the next detected irrigation, or at 48 h, whichever occurred first. Observations after the first reference crossing were not allowed to re-enter the fitted window. Retained windows required at least eight observations, at least six hours of duration, and a peak rise of at least 2 percentage points. These operational criteria define a selected subpopulation of clear recoveries.

2.3 Positive-state model

Let $\theta(h) > 0$ denote the sensor-reported moisture at elapsed time $h \geq 0$ after the selected peak and let $\theta_{\text{ref}} > 0$ be the event reference. Define

$$y_\rho(t) = \frac{\theta(h)}{\theta_{\text{ref}}}, \qquad t = 1 + \frac{h}{h_0}, \qquad h_0 > 0. \tag{1}$$

The equilibrium is $y_\rho = 1$. For u, v, $c > 0$, the proportional operations used here are

$$u \oplus v = uv, \qquad c \odot u = \exp\{(\log c)(\log u)\}. \tag{2}$$

With $x = \log t$ and $Y(x) = \log y_\rho(e^x)$, the proportional derivative is $D_\rho y_\rho(t) = \exp\{Y'(\log t)\}$. The first-order unforced law is

$$D_\rho y_\rho(t) \oplus a \odot y_\rho(t) = 1, \qquad y_\rho(1) = y_0 > 0, \tag{3}$$

where $a = e^\alpha$ and $\alpha > 0$. Logarithmic coordinates give $Y'(x) + \alpha Y(x) = 0$, hence

$$\theta_\rho(h) = \theta_{\text{ref}} \exp\left\{\log\left(\frac{\theta_0}{\theta_{\text{ref}}}\right)\left(1 + \frac{h}{h_0}\right)^{-\alpha}\right\}. \tag{4}$$

Thus

$$\left|\log \frac{\theta_\rho(h)}{\theta_{\text{ref}}}\right| = \left|\log \frac{\theta_0}{\theta_{\text{ref}}}\right| \left(1 + \frac{h}{h_0}\right)^{-\alpha}. \tag{5}$$

Specifically, the logarithmic relative deviation exhibits power-law decay in shifted time; the moisture percentage itself does not follow a pure power law.

Differentiating Eq. (4) gives the ordinary equation

$$\frac{d\theta}{dh} = -\frac{\alpha}{h + h_0}\,\theta(h) \log\left(\frac{\theta(h)}{\theta_{\text{ref}}}\right). \tag{6}$$

The equilibrium $\theta = \theta_{\text{ref}}$ is globally attracting on the positive state space. The time required to halve the logarithmic relative deviation is

$$h_{1/2} = h_0\left(2^{1/\alpha} - 1\right). \tag{7}$$

2.4 Comparator models

All models shared the same fixed θ_{ref}, peak anchor θ_0, observations, and log-ratio loss. Besides Eq. (4), the prespecified set was

$$\theta_{\text{AP}}(h) = \theta_{\text{ref}} + (\theta_0 - \theta_{\text{ref}})\left(1 + \frac{h}{h_0}\right)^{-\beta}, \qquad \beta > 0, \tag{8}$$

$$\theta_{\exp}(h) = \theta_{\text{ref}} + (\theta_0 - \theta_{\text{ref}})e^{-kh}, \qquad k > 0, \tag{9}$$

$$\theta_{\text{SE}}(h) = \theta_{\text{ref}} + (\theta_0 - \theta_{\text{ref}}) \exp\left(-\left(\frac{h}{\tau}\right)^{\gamma}\right), \qquad \tau, \gamma > 0. \tag{10}$$

For a small initial relative deviation $\delta_0 = (\theta_0 - \theta_{\text{ref}})/\theta_{\text{ref}}$, Eq. (4) has the first-order approximation

$$\theta_\rho(h) = \theta_{\text{ref}} + (\theta_0 - \theta_{\text{ref}})\left(1 + \frac{h}{h_0}\right)^{-\alpha} + O(\delta_0^2), \tag{11}$$

which explains why proportional and additive-power curves may be difficult to distinguish empirically.

2.5 Estimation, diagnostics, and validation

The base analysis fixed $h_0 = 6$ h. Positive parameters were estimated by deterministic, bounded minimization of the squared log-ratio residuals. The stretched exponential was fitted using deterministic, bounded multistart optimization. Optimizer convergence and boundary flags were retained.

The primary metric was the root mean squared log-ratio error ($\text{RMSE}_{\log}$):

$$\text{RMSE}_{\log} = \left\{\frac{1}{n}\sum_{i=1}^{n}\left[\log\left(\frac{\theta_{\text{obs},i}}{\theta_{\text{pred},i}}\right)\right]^2\right\}^{1/2}. \tag{12}$$

Secondary diagnostics were original-scale root mean squared error (RMSE), mean absolute relative error (MARE), mean log residual, lag-1 residual autocorrelation (ACF1), and corrected Akaike information criterion (AICc), computed from the log-error sum of squared errors (SSE) with one fitted parameter for the proportional, additive-power, and exponential curves and two for the stretched exponential. AICc was used only as a descriptive, complexity-adjusted comparison because θ_{ref} and θ_0 were preprocessing anchors.

For ordered-time hold-out, models were fitted to observations in the first 70% of elapsed recovery duration and scored on the final 30%, requiring at least six training and three validation points. This procedure evaluates internal temporal extrapolation rather than external validation. Paired counts and medians were reported without event-level sign-test p values or independent and identically distributed (IID) bootstrap intervals because all events came from one serially observed farm.

Sensitivity analyses varied h_0 (3, 6, 12 h), shifted θ_{ref} by ±0.5 percentage points, changed the water threshold (200, 300, 400 L), varied the flow-increment threshold (0, 1, 5, 10 L), and replaced the observed peak by a local median within ±20 min. The public release includes all event traces and sensitivity outputs.

3. Results

3.1 Input audit and event screening

The audit retained all 4,293 moisture and 17,427 valve rows. Two rows shared one flow timestamp; deterministic duplicate resolution reduced the flow series from 17,411 to 17,410 rows. No non-finite records were removed. Two large positive flow increments were flagged for review, and no negative differences were used as irrigation input.

The 5 L rule produced 101 irrigation events, 70 of which delivered at least 300 L. Thirty-six events (35.6%) satisfied all criteria (Table I). Retained events had larger median water volume (1126.7 vs 390.7 L), longer irrigation duration (52.5 vs 25.0 min), greater moisture rise (8.16 vs 2.86 percentage points), and longer usable recovery duration (9.63 vs 1.33 h) than excluded events. These differences indicate that the analysis focuses on a selected high-signal subset.

Figure 1.

Sensor-reported soil-moisture percentage over the study period. Shaded intervals indicate flow-derived events with at least 300 L under the canonical > 5 L increment rule.

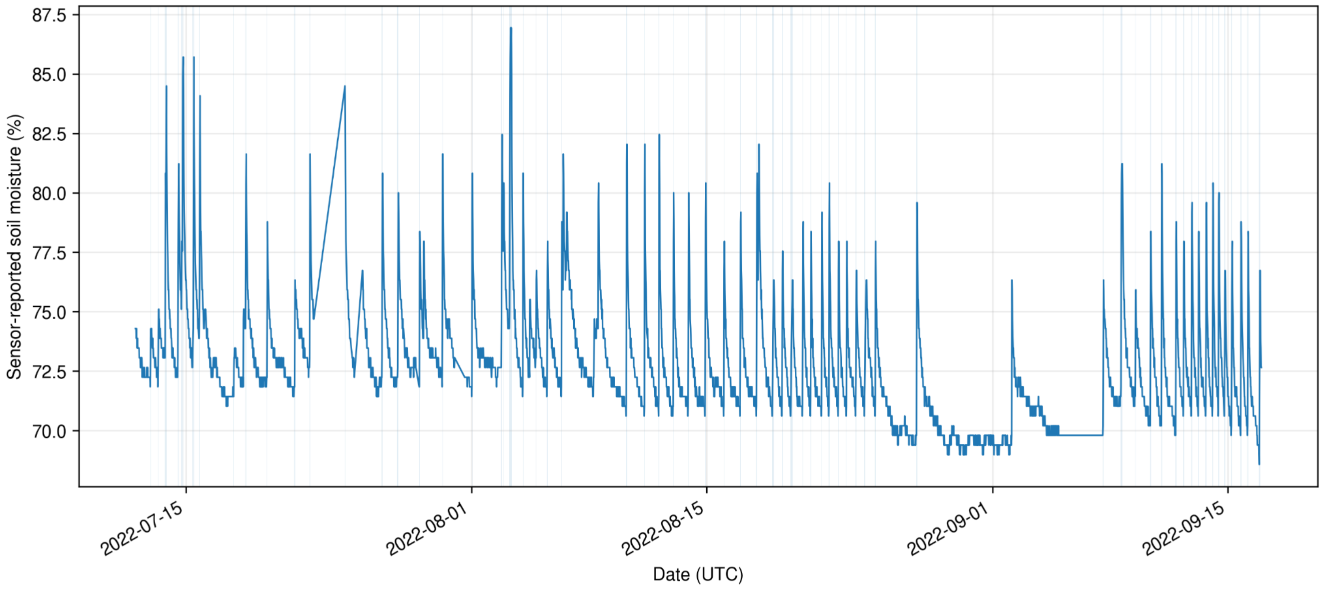

Table I

Mutually exclusive event-screening trace under the canonical protocol.

Stage	Excluded	Remaining	Remaining (%)
Flow-derived irrigation events detected	0	101	100.0
Applied water below 300 L	31	70	69.3
Insufficient pre-event baseline	3	67	66.3
Insufficient post-irrigation peak search	3	64	63.4
Rise below 2 percentage points or invalid reference	0	64	63.4
Fewer than 8 contiguous above-reference observations	8	56	55.4
Contiguous above-reference duration below 6 h	20	36	35.6

3.2 Full-window model comparison

Table II shows that the proportional and additive-power curves had similar median error, whereas the one-parameter exponential performed less well and exhibited stronger residual autocorrelation. The stretched exponential had the lowest median full-window error and nearly zero median residual autocorrelation. It yielded the lowest $RMSE_{log}$ in 33 of 36 events and the lowest AICc in 27 events. The proportional curve yielded the lowest $RMSE_{log}$ in only three events, although it had lower error than the exponential and additive power in 32 events each.

Paired differences clarify the scale of these comparisons (Table III). Against additive power, the median full-window improvement of the proportional model was only 8.5×10^{-5} in $RMSE_{log}$. Against the exponential, the corresponding difference was 0.00220. Against the stretched exponential, the median difference was negative, favoring the stretched curve by 0.00078.

3.3 Ordered-time hold-out and parameter summaries

All 36 retained events met the elapsed-time split requirements. The proportional curve outperformed the exponential in 29 hold-outs and additive power in 22. The proportional and stretched exponential each performed better in 18 events, with nearly identical median hold-out $RMSE_{log}$ values (0.00317 and 0.00315). This result tempers the full-window ranking: the stretched exponential provides greater in-sample flexibility, while its median extrapolation advantage was negligible under this internal split-sample evaluation.

The median proportional exponent was 2.589 (IQR 2.095–3.107), corresponding to a median $h_{1/2}$ of 1.842 h. The median additive-power exponent was 2.667, the median exponential rate was 0.345 per hour, and the stretched-exponential medians were $\tau = 2.559$ h and $\gamma = 0.735$. These are event-level descriptive parameters tied to the preprocessing definition and should not be interpreted as transferable soil properties.

3.4 Protocol sensitivity

The flow-increment sensitivity produced 134 detected events at a 0 L threshold, 104 at 1 L, 101 at 5 L, and 100 at 10 L; retained counts were 34, 36, 36, and 37, respectively. Thus, the 5 L threshold filters out numerous small counter increments while yielding a retained sample similar to that obtained with

Table II

Full-window descriptive model summary across the 36 retained events. RMSE on the original scale is in sensor percentage points; MARE denotes mean absolute relative error, ACF1 denotes residual autocorrelation at lag 1, and AICc denotes the corrected Akaike information criterion.

Model	Median RMSElog	Median RMSE	Median MARE	Median ACF1	Best RMSE	Best AICc
Proportional	0.00351	0.259	0.00274	0.350	3	5
Additive power	0.00360	0.267	0.00282	0.369	0	0
Additive exponential	0.00597	0.443	0.00492	0.742	0	4
Stretched exponential	0.00298	0.217	0.00233	0.013	33	27

Figure 2.

Event-level paired differences in full-window log-ratio RMSE. Positive values favor the proportional curve; negative values favor the named comparator. Events are ordered by exponentialminus-proportional difference.

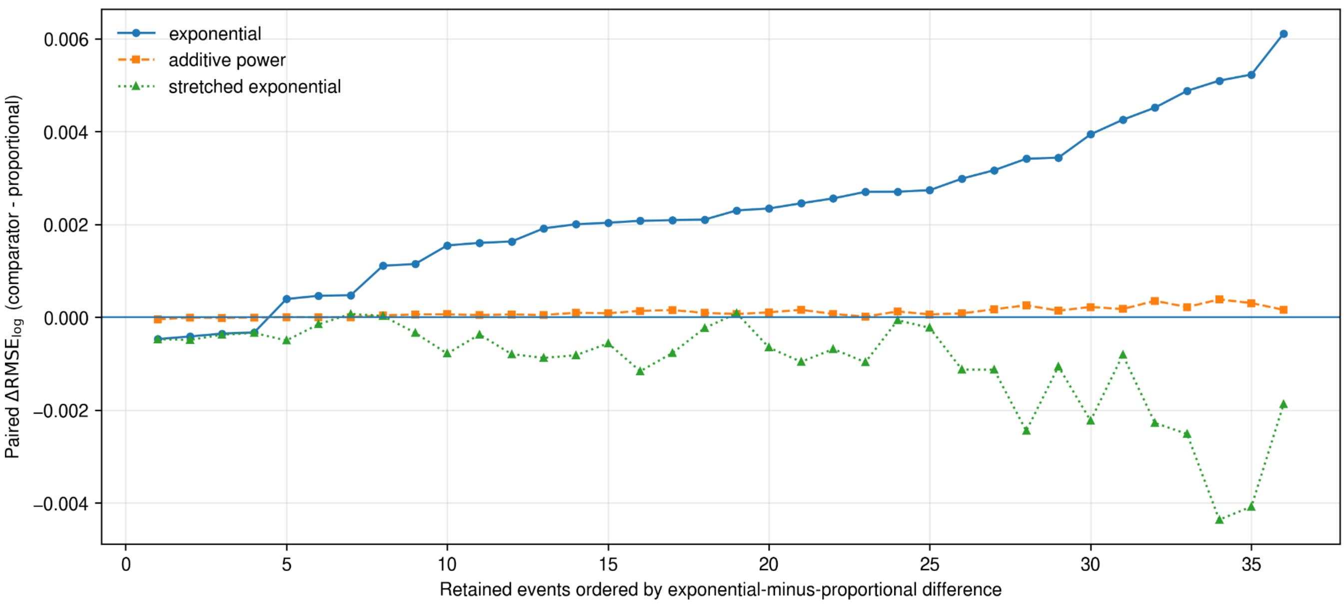

the 1 L threshold. Applied-water thresholds of 200, 300, and 400 L all yielded the same 36 retained events because the additional lower-volume events failed later criteria.

Changing h_0 to 3 or 12 h left the proportional-versus-exponential win count at 32/36 but changed the median α from 1.549 to 4.619. Shifting θ_{ref} down by 0.5 percentage points produced 33/36 proportional wins versus the exponential, whereas shifting it up by 0.5 reduced the count to 27/36. The robust local-median peak rule retained 34 events and produced 26 proportional wins versus the exponential, compared with 32/36 under the observed-maximum rule. These changes demonstrate that the reference and peak definitions are integral to the estimand.

3.5 Illustrative event

Event 15 delivered 935.3 L, had $\theta_{ref} = 72.24\%$, $\theta_0 = 77.96\%$, and retained 72 observations over 23.57 h before the first reference crossing. The fitted proportional exponent was 1.894 and $h_{1/2} = 2.65$ h. Full-window $\text{RMSE}_{\log}$ values were 0.00306 (proportional), 0.00312 (additive power), 0.00580 (exponential), and 0.00283 (stretched exponential). Residual ACF1 values were 0.318, 0.342, 0.777, and 0.195, respectively.

4. Discussion

4.1 Defensible contribution and model ranking

The proportional formulation defines a positive state, an equilibrium represented by the ratio 1, an exact linear law for the logarithmic representative, and the interpretable half-reduction time in Eq. (7). Equation (6) also shows that the same trajectory can be represented by an ordinary non-autonomous relaxation. The contribution is therefore a coherent positive-state parameterization and error geometry, not a claim that classical analysis cannot express the curve.

Table III

Paired descriptive comparisons. Differences are comparator minus proportional, so positive values favor the proportional curve.

Analysis	Comparator	Events	Prop. lower	Median prop./comp.	Median difference
Full window	Additive power	36	32	0.00351 / 0.00360	0.000085
Full window	Additive exponential	36	32	0.00351 / 0.00597	0.002203
Full window	Stretched exponential	36	3	0.00351 / 0.00298	−0.000778
Ordered-time hold-out	Additive power	36	22	0.00317 / 0.00324	0.000044
Ordered-time hold-out	Additive exponential	36	29	0.00317 / 0.00534	0.002215
Ordered-time hold-out	Stretched exponential	36	18	0.00317 / 0.00315	−0.000025

Figure 3.

Event 15. (a) Identical observations fitted by all four candidate curves; open circles and crosses denote training and validation portions under the elapsed-time split. (b) Log-ratio residuals. This event is presented for illustration only and was not randomly selected.

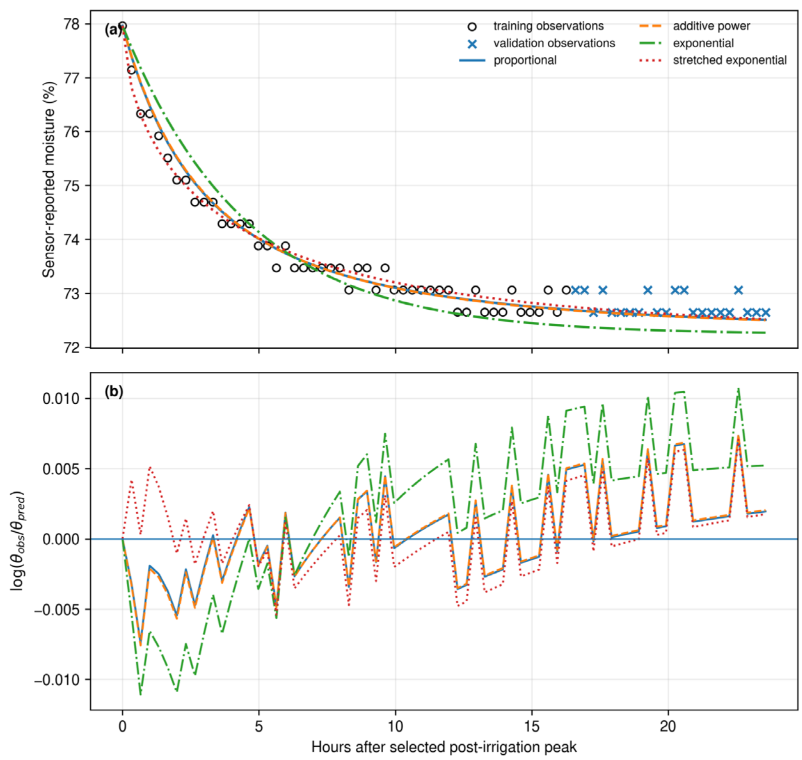

The full benchmark alters the empirical interpretation. The proportional curve consistently outperformed a simple additive exponential for most retained events, but its advantage over a freely fitted additive power law was very small. The stretched exponential was the best full-window descriptor in most events and substantially reduced the residual autocorrelation. However, proportional and stretched-exponential hold-out performance was evenly split. This provides a more informative scientific comparison than a favorable two-model comparison: the dataset supports slow-tailed recovery and shows that no single curve is unambiguously dominant under both fit and internal extrapolation criteria.

4.2 Selection, reference dependence, and residual structure

Only 36 of 101 detected events entered the analysis. Retained events had stronger pulses, larger rises, and longer recoveries, so the results cannot be generalized to all irrigations. The retrospectively selected maximum may be sensitive to noise, while the strict first-crossing rule conditions the sample on remaining above θ_{ref}. These choices reduce the earlier risk of noncontiguous re-entry but do not eliminate selection bias.

Reference sensitivity was substantial. A 0.5-percentage-point change in θ_{ref} altered both fitted geometry and win counts, and the robust peak rule changed the retained sample. Future work should define the reference independently when possible, model the baseline trend, and propagate reference and peak uncertainty jointly. Residual ACF1 also shows that pointwise errors are serially dependent; event-level RMSE and AICc are descriptive summaries, not evidence of independent Gaussian errors.

4.3 Measurement and external validity

The reported sensor percentage has not been established as calibrated volumetric water content. Original-scale errors therefore refer only to percentage points of the recorded sensor output and cannot be converted into soil-water storage. Rainfall, temperature, radiation, humidity, wind, evapotranspiration, root uptake, and spatial redistribution were unavailable. Fitted parameters may absorb these omitted processes and must not be interpreted as hydraulic conductivity or causal irrigation effects.

The ordered-time split evaluates extrapolation within the same selected event and is not external validation. A stronger study should hold out complete events by later period, sensor, field, soil, crop, or farm; include weather and irrigation covariates; and use hierarchical or blocked inference when genuine replication exists. Accordingly, the present work should be interpreted as a reproducible methodological case study in agricultural sensor analysis, not as an operational irrigation rule.

4.4 Reproducibility and limitations of the repository release

Version 1.2.0 is the sole analytical implementation for this study. It reproduces the 101 detected and 36 retained events, all four models, strict windows, sensitivity tables, and figures from one command. Regression tests verify exact event identifiers and prevent recurrence of noncontiguous re-entry after the first reference crossing. The immutable software archive, checksums, configuration, and machine-readable provenance make the reported analysis independently auditable and reduce the risk of method-code drift.

5. Conclusions

The proportional positive-state law is a mathematically coherent and interpretable parameterization of recovery toward a positive reference. In 36 selected events from one open single-site dataset, it performed better than a simple additive exponential and similarly to a fitted additive power law. A stretched exponential gave lower full-window error in most events, while its ordered-time hold-out performance was essentially tied with the proportional curve.

The defensible contribution is therefore not universal predictive superiority. It is the combination of a positive reference-ratio formulation, explicit links to ordinary and power-law models, strict event-window definitions, transparent reporting of unfavorable comparative evidence, and a reproducible workflow. Agronomic or operational use requires calibrated measurements, independently defined references, uncertainty propagation, relevant environmental covariates, and multi-site external validation.

Acknowledgments

The authors acknowledge Manzano et al. (Manzano et al., 2023) for releasing the smart-irrigation dataset under CC BY 4.0. The authors thank their institutions for academic support during the preparation of this manuscript.

Declarations

Funding. M.M.L.-F. received partial funding from project EVAAT-GCN under FINEP agreement 01.24.0661.00, ref. 3311/24.

Competing interests. The authors declare no competing interests.

Ethics approval. Not applicable. The study reused an openly licensed agricultural sensor dataset and involved no new sampling of humans or animals.

Consent to participate. Not applicable.

Consent for publication. Not applicable.

Data availability. The raw data are available from Mendeley Data, Version 3, https://doi.org/10.17632/cjb4vy4mzj.3, under CC BY 4.0. The exact configuration, derived event tables, figures, software environment, and machine-readable provenance are supplied in the accompanying software release v1.2.0. The public GitHub mirror and the immutable Zenodo version DOI will be added to the final submission metadata after deposition; the deposited tag will be identical to the supplied release.

Code availability. The analysis code is MIT licensed. Repository-authored documentation and results are CC BY 4.0, while the bundled source dataset retains its original CC BY 4.0 license. The archived release reconstructs all reported

tables and figures with the documented command.

Materials availability. Not applicable.

Author contributions. G.A.M.-B.: conceptualization, investigation, methodology, software, formal analysis, visualization, writing–original draft, and writing–review and editing. M.M.L.-F.: conceptualization, investigation, formal analysis, validation, and writing–review and editing. W.C.-L.: conceptualization, methodology, validation, supervision, project administration, and writing–review and editing.

Use of generative AI assistance. Generative AI tools were used as described in Materials and Methods. The authors verified and accept responsibility for all content.

References

Allen RG, Pereira LS, Raes D, Smith M (1998) Crop evapotranspiration: Guidelines for computing crop water requirements. FAO Irrigation and Drainage Paper 56. FAO, Rome. https://www.fao.org/4/x0490e/x0490e00.htm Bashirov

AE, Kurpinar EM, Ozyapici A (2008) Multiplicative calculus and its applications. Journal of Mathematical Analysis and Applications 337(1):36–48. https://doi.org/10.1016/j.jmaa.2007.03.081

Bittelli M (2011) Measuring soil water content: A review. HortTechnology 21(3):293–300. https://doi.org/10.21273/HORTTECH.21.3.293

Campillay-Llanos WA, Guevara F, Pinto M, Torres R (2021) Differential and integral proportional calculus: how to find a primitive for $f(x) = 1/\sqrt{2\pi}\ e^{-x^2/2}$. International Journal of Mathematical Education in Science and Technology 52(3):463–476. https://doi.org/10.1080/0020739X.2020.1763489

Datta S, Taghvaeian S (2023) Soil water sensors for irrigation scheduling in the United States: A systematic review of literature. Agricultural Water Management 278:108148. https://doi.org/10.1016/j.agwat.2023.108148

Ganjegunte GK, Sheng Z, Clark JA (2012) Evaluating the accuracy of soil water sensors for irrigation scheduling to conserve freshwater. Applied Water Science 2:119–125. https://doi.org/10.1007/s13201-012-0032-7

Gong M, Killick R, Nemeth C, Quinton J (2025) A changepoint approach to modeling nonstationary soil moisture dynamics. Journal of the Royal Statistical Society Series C: Applied Statistics 74(3):866–883. https://doi.org/10.1093/jrsssc/qlaf004

Jones HG (2004) Irrigation scheduling: advantages and pitfalls of plant-based methods. Journal of Experimental Botany 55(407):2427–2436. https://doi.org/10.1093/jxb/erh213

Manzano JM, Orihuela L, Tapia Córdoba A, Pacheco E, Bareiro J (2023) Smart irrigation control system data with soil moisture, flow meter and electrovalve relay. Mendeley Data, Version 3. https://doi.org/10.17632/cjb4vy4mzj.3

McColl KA, Wang W, Peng B, Akbar R, Short Gianotti DJ, Lu H, Pan M, Entekhabi D (2017) Global characterization of surface soil moisture drydowns. Geophysical Research Letters 44:3682–3690. https://doi.org/10.1002/2017GL072819

Orihuela L, Pacheco E, Bareiro J, Tapia A, Manzano JM (2025) Deployment of a smart irrigation control system with capacity-based moisture sensors on a production farm. Journal of Irrigation and Drainage Engineering 151(1):04024039. https://doi.org/10.1061/JIDEDH.IRENG-10124

Raoult N, Ottlé C, Peylin P, Bastrikov V, Maugis P (2021) Evaluating and optimizing surface soil moisture drydowns in the ORCHIDEE land surface model at in situ locations. Journal of Hydrometeorology 22:1025–1043. https://doi.org/10.1175/JHM-D-20-0115.1

Richards LA (1931) Capillary conduction of liquids through porous mediums. Physics 1:318–333. https://doi.org/10.1063/1.1745010

Sehgal V, Gaur N, Mohanty BP (2021) Global surface soil moisture drydown patterns. Water Resources Research 57:e2020WR027588. https://doi.org/10.1029/2020WR027588

Sinha J, Sharma A, Marshall L, Kim S (2024) Characterizing satellite soil moisture drydown: A bivariate filtering approach. Water Resources Research 60(7):e2022WR034019. https://doi.org/10.1029/2022WR034019

Topp GC, Davis JL, Annan AP (1980) Electromagnetic determination of soil water content: Measurements in coaxial transmission lines. Water Resources Research 16(3):574–582. https://doi.org/10.1029/WR016i003p00574

Vereecken H, Huisman JA, Bogena H, Vanderborght J, Vrugt JA, Hopmans JW (2008) On the value of soil moisture measurements in vadose zone hydrology: A review. Water Resources Research 44:W00D06. https://doi.org/10.1029/2008WR006829